Dynamic modelling and small signal analysis of push-pull bidirectional DC-DC converter

Hongjuan Zhang, Long Quan*, Yan Gao

Key Lab of Advanced Transducers and Intelligent Control System, Ministry of Education, Taiyuan University of Technology, Taiyuan 030024, China

Received 1 April 2014, www.cmnt.lv

Abstract

Bidirectional DC-DC converter can not only act as a contact bridge between two different voltage levels systems, but also can achieve the energy flow in both directions. However, due to the operating characteristics of the active switch and diode in the converter, thereby the inverter becomes a strong nonlinear circuit. In light of this, the push-pull bidirectional DC-DC converter is designed and the method of state space small signal analysis is proposed. First of all, the state-space equations of the converter are established. Then each variable of inverter circuit is averaged in a switching cycle to eliminate the influence of the switching ripple. The respective average variable expressions are decomposed into the DC component and AC small signal component. After the DC component of the signal is eliminated, the expression of the AC small signal component is obtained, to achieve the purpose of separating the small signal. Finally, the expression of small signal component is linearized, thereby the nonlinear system is approximated the DC operating point. This study will provide the theoretical foundation ready for the analysis and design of converter controller.

Keywords: dynamic modelling, state space averaging method, small signal analysis, linearization

1 Introduction

As the development of the new energy technology, transmission technology, the power supply technology and motor driver technology, the bidirectional DC-DC (Direct Current to Direct Current) converter technology becomes a new branch of power electronic technology. Not only the bidirectional DC-DC converter can transform the voltage, but also can achieve two-way power flow. So it has been widely used in all kinds of occasions. At the same time, it also becomes a research hotspot [1].

The isolated bidirectional DC-DC converter is a kind indirect transform circuit, which consists of the inverter link, high-frequency transformer and rectifier. Because the push-pull converter has many advantages of simple structure, transformer winding bidirectional excitation, the small switch conduction loss and simple drive circuit, that it is widely used in small and medium power switching power supply [2]. In the DC converter working process, due to the active switching devices and diodes in converter is working in a wide range of its characteristic curve, so that the converter is a strong nonlinear circuit. In order to improve the control performance, work efficiency, and reduce loss, many scholars have done a lot of research in domestic and foreign countries [3]. The several typical topologies of isolated bidirectional DC-DC converters were presented. And the circuit structure and working principle were analysed [4]. The ZVS push-pull resonant converter has been proposed and the half bridge rectifier has been adopted in the second of transformer [5]. The bidirectional isolated DC-DC converter has been presented, combined push-pull-forward circuit, half-bridge circuit with high-frequency transistors [6]. The state feedback control of push-pull DC-DC converter has been proposed by frequency-domain conditions based on the Hermite-Biehler theorem, and the robust stability has been analysed [7]. A resonant isolation push-pull converter was investigated. In order to improve the system efficiency, a switching loss analysis was performed [8].

In the above analysis and research, the full bridge rectifiers are adopted in the rectifier link of the push-pull bi-directional DC-DC converter, or the half bridge rectifiers are used. More switching devices are used in circuit. And the converters are mainly applied in DC power output voltage above 100V. In view of the energy needs of two-way conversion in the medium power applications, a push-pull bi-directional DC-DC converter is designed in the paper. The topology of each variable in a switch period of work modal is analysed. The analysis method of the state space small signal is adopted. The AC (Alternation Current) small signal state space expression of push-pull bidirectional DC-DC converter is established and is linearized. These works lay the foundation for the further design of control model.

2 Working principle and dynamic modelling

The push-pull isolated bidirectional DC-DC converter introduces a pair of symmetrical switches in the output terminal of common push-pull DC-DC converter. So the both ends of the circuit structure become symmetry, and the two-way flow of energy can be realized. Figure 1 below shows the push-pull bidirectional DC/DC converter.

* ***Corresponding author*** e-mail: quanlong@tyut.edu.cn

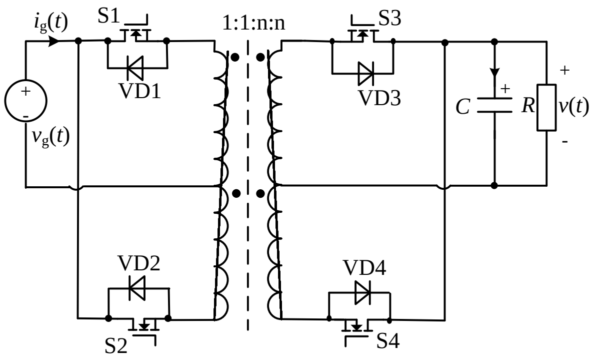

FIGURE 1 Push-pull bidirectional DC-DC converter

In order to realize the two-way flow of energy, the converter must operate in continuous mode. When the energy transmitted from the left side to the right side, the converter has four kinds of switch modes in a switch period. The switch S1 and S2 alternately turn on and respectively formed the opposite phase AC voltage in the side of two windings. When the switch S1 is turned on, the diode VD3 is in conducting state. When the switch S2 is turned on, the diode VD4 is in conducting state. When the two switches are turned off, the diode VD3 and VD4 are all in the on state, each shares a half of the current. When the energy transmitted from the right side to the left side, the working state is same with the above situation because of the circuit symmetry. When the switch S3 is turned on, the diode VD1 is in conducting state. When the switch S4 is turned on, the diode VD2 is in conducting state. When the two switches are turned off, the diode VD1 and VD2 are all in the on state, each shares a half of the current.

The magnetizing inductance of transformer is involved in energy transfer, so the actual transformer is replaced by the magnetizing inductance and the ideal transformer parallel model. Considering the internal resistance of magnetizing inductance, the analysis circuit of push-pull bidirectional DC-DC converter is shown in Figure 2.

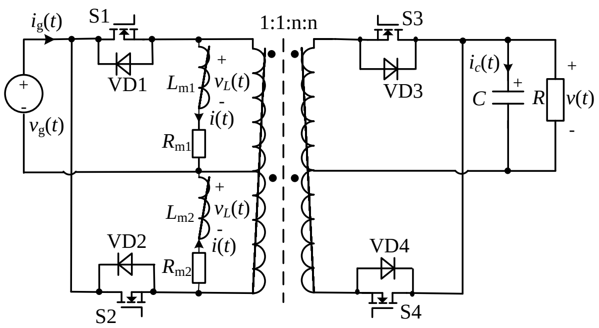

FIGURE 2 Analysis circuit of push-pull bidirectional DC-DC converter

The timing control rules of switch driving in the push-pull bidirectional DC-DC converter are shown in Figure 3. The duty ratio $d(t)$ is a controlled variable and is defined as the conduction time and the cycle ratio, $d(t)=t_{on}/T_s$. According to the control law of the switch, the state equations of the converter are calculated in four kinds of operating condition. The inductor current $i(t)$ and $v(t)$ capacitor voltage are selected as the state vector, and the state vector is expressed for $x(t)=[i(t),\ v(t)]^T$. The input current $i_g(t)$ and the output voltage $v(t)$ are used as the output vector, and the output vector is expressed for $y(t)=[i_g(t),\ v(t)]^T$. The input voltage $v_g(t)$ is uses as the input vector, and the input vector is expressed for $u(t)=[v_g(t)]$.

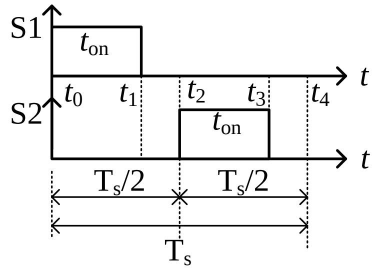

FIGURE 3 Switching sequence of S1 and S2

The working mode 1: t_0~t_1 time interval is for $[0, d(t)T_s]$. In this period, the switch S1 is turned on, and the diode VD3 is on state. The current flows through the transformer, diode VD3, a filter capacitor C and load R. At the same time the current value increases. The topological structure is shown in Figure 4 in this period. Due to symmetry circuit, a magnetizing inductances are supposed for $L_{m1}=L_{m2}=L_m$, and the inductive resistances are supposed for $R_{m1}=R_{m2}=R_m$.

The state equation is expressed for:

$$\begin{cases} v_L(t)=L_m\dfrac{di(t)}{dt}=v_g(t)-i(t)R_m \\ i_c(t)=C\dfrac{dv(t)}{dt}=\dfrac{i(t)}{n}-\dfrac{v(t)}{R} \end{cases}. \qquad (1)$$

The output equation is expressed for:

$$\begin{cases} i_g(t)=i(t) \\ v(t)=v(t) \end{cases}. \qquad (2)$$

Can be derived for:

$$\begin{cases} \dot{x}(t)=\begin{bmatrix}\dot{i}(t)\\ \dot{v}(t)\end{bmatrix}=A_1\begin{bmatrix}i(t)\\ v(t)\end{bmatrix}+B_1\begin{bmatrix}v_g(t)\end{bmatrix} \\ y(t)=\begin{bmatrix}i_g(t)\\ v(t)\end{bmatrix}=C_1\begin{bmatrix}i(t)\\ v(t)\end{bmatrix}+E_1\begin{bmatrix}v_g(t)\end{bmatrix} \end{cases}, \qquad (3)$$

where $A_1=\begin{bmatrix}-\dfrac{R_m}{L_m} & 0 \\ \dfrac{1}{nC} & -\dfrac{1}{RC}\end{bmatrix}$, $B_1=\begin{bmatrix}\dfrac{1}{L_m}\\ 0\end{bmatrix}$, $C_1=\begin{bmatrix}1 & 0\\ 0 & 1\end{bmatrix}$, $E_1=\begin{bmatrix}0\\ 0\end{bmatrix}$.

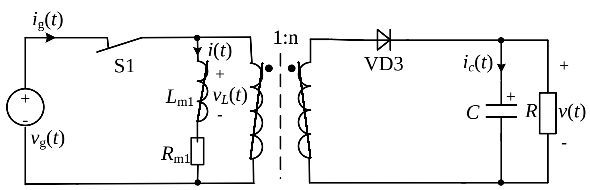

FIGURE 4 Topological structure in t_0~t_1

The working mode 2: t_1~t_2 time interval is for [$d(t)$T$_s$, T$_s$/2]. In this period, the switches S1 and S2 are turned off. The freewheeling current flows through the diode VD3 and the diode VD, The current value is respectively half of total current. At the same time the current value decreases. The topological structure is shown in Figure 5 in this period.

The state equation is expressed for:

$$\begin{cases} v_L(t) = L_m \dfrac{di(t)}{dt} = \dfrac{v(t)}{n} - i(t)R_m \\ i_c(t) = C\dfrac{dv(t)}{dt} = \dfrac{i(t)}{n} - \dfrac{v(t)}{R} \end{cases}. \quad (4)$$

The output equation is expressed for:

$$\begin{cases} i_g(t) = 0 \\ v(t) = v(t) \end{cases}. \quad (5)$$

Can be derived for:

$$\begin{cases} \dot{x}(t) = \begin{bmatrix} \dot{i}(t) \\ \dot{v}(t) \end{bmatrix} = A_2 \begin{bmatrix} i(t) \\ v(t) \end{bmatrix} + B_2 \begin{bmatrix} v_g(t) \end{bmatrix} \\ y(t) = \begin{bmatrix} i_g(t) \\ v(t) \end{bmatrix} = C_2 \begin{bmatrix} i(t) \\ v(t) \end{bmatrix} + E_2 \begin{bmatrix} v_g(t) \end{bmatrix} \end{cases}. \quad (6)$$

where $A_2 = \begin{bmatrix} -\dfrac{R_m}{L_m} & \dfrac{1}{nL_m} \\ \dfrac{1}{nC} & -\dfrac{1}{RC} \end{bmatrix}$, $B_2 = \begin{bmatrix} 0 \\ 0 \end{bmatrix}$, $C_2 = \begin{bmatrix} 0 & 0 \\ 0 & 1 \end{bmatrix}$, $E_2 = \begin{bmatrix} 0 \\ 0 \end{bmatrix}$.

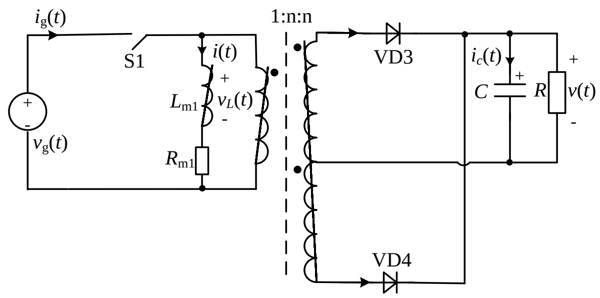

FIGURE 5 Topological structure in t_1~t_2

The working mode 3: t_2~t_3 time interval is for [T_s/2, T_s/2+$d(t)T_s$]. In this period, the switch S2 is turned on, and the diode VD4 is on state. The current flows through the transformer, diode VD4, a filter capacitor C and load R. At the same time the current value increases. The topological structure is shown in Figure 6 in this period.

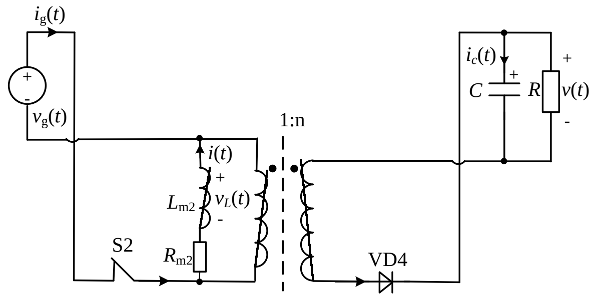

FIGURE 6 Topological structure in t_2~t_3

Due to the symmetry of the circuit, the state equation and output equation are expressed for:

$$\begin{cases} \dot{x}(t) = \begin{bmatrix} \dot{i}(t) \\ \dot{v}(t) \end{bmatrix} = A_3 \begin{bmatrix} i(t) \\ v(t) \end{bmatrix} + B_3 \begin{bmatrix} v_g(t) \end{bmatrix} \\ y(t) = \begin{bmatrix} i_g(t) \\ v(t) \end{bmatrix} = C_3 \begin{bmatrix} i(t) \\ v(t) \end{bmatrix} + E_3 \begin{bmatrix} v_g(t) \end{bmatrix} \end{cases}, \quad (7)$$

where A_3=A_1, B_3=B_1, C_3=C_1, E_3=E_1.

The working mode 4: t_2~t_3 time interval is for [T_s/2+$d(t)T_s$, T_s]. In this period, the work state is like the work mode 2. The topological structure is shown in Figure 7 in this period.

The state equation and output equation are expressed for:

$$\begin{cases} \dot{x}(t) = \begin{bmatrix} \dot{i}(t) \\ \dot{v}(t) \end{bmatrix} = A_4 \begin{bmatrix} i(t) \\ v(t) \end{bmatrix} + B_4 \begin{bmatrix} v_g(t) \end{bmatrix} \\ y(t) = \begin{bmatrix} i_g(t) \\ v(t) \end{bmatrix} = C_4 \begin{bmatrix} i(t) \\ v(t) \end{bmatrix} + E_4 \begin{bmatrix} v_g(t) \end{bmatrix} \end{cases}. \quad (8)$$

where A_4=A_1, B_4=B_1, C_4=C_1, E_4=E_1:

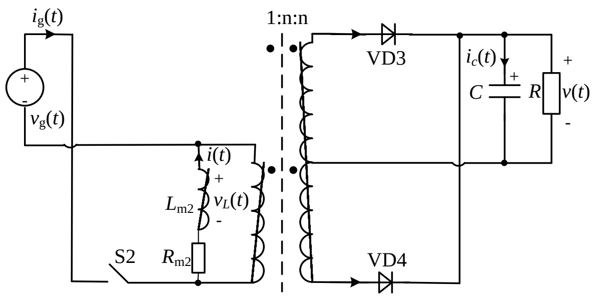

FIGURE 7 Topological structure in t_3~t_4

3 Average state vector

In order to eliminate the influence of the switching ripple, it is necessary that the state variables are averaged in a switching period, and the average state variables equations are established. The average state vectors are defined as:

$$\langle \dot{x}(t)\rangle_{T_s} = \frac{d}{dt}\langle x(t)\rangle_{T_s} = \frac{d}{dt}\left(\frac{1}{T_s}\int_t^{t+T_s} x(\tau)d\tau\right) = \frac{1}{T_s}\int_t^{t+T_s}\dot{x}(\tau)d\tau = \frac{1}{T_s}\left\{\int_t^{t+d(t)T_s}\dot{x}(\tau)d\tau + \int_{t+d(t)T_s}^{t+T_s/2}\dot{x}(\tau)d\tau + \int_{t+T_s/2}^{t+T_s/2+d(t)T_s}\dot{x}(\tau)d\tau + \int_{t+T_s/2+d(t)T_s}^{t+T_s}\dot{x}(\tau)d\tau\right\}. \quad (9)$$

The Equations (3), (6)-(8) are substituted into equation (9) and then the following expression can be obtained:

$$\langle \dot{x}(t)\rangle_{T_s} = \frac{1}{T_s}\left\{\int_t^{t+d(t)T_s}[A_1x(\tau)d\tau + B_1u(t)]d\tau + \int_{t+d(t)T_s}^{t+T_s/2}[A_2x(\tau)d\tau + B_2u(t)]d\tau + \int_{t+T_s/2}^{t+T_s/2+d(t)T_s}[A_3x(\tau)d\tau + B_3u(t)]d\tau + \int_{t+T_s/2+d(t)T_s}^{t+T_s}[A_4x(\tau)d\tau + B_4u(t)]d\tau\right\}. \quad (10)$$

When the converter to meet the low frequency hypothesis and small ripple hypothesis, with respect to the state variables and input variables can be replaced with the instantaneous value of average value in a switching period, and they can be regarded as the average to maintain the constant value in a switching period. These treatments can not introduce large error analysis. So the state variables $\langle x(t)\rangle_{Ts}$ and $\langle u(t)\rangle_{Ts}$ can be regarded as constants in a switching period. Then the Equation (10) can be approximately simplified and inferred. The expressions of average state variable equation are obtained:

$$\langle \dot{x}(t)\rangle_{T_s} = [2d(t)\cdot A_1 + (1-2d(t)\cdot A_2]\langle x(t)\rangle_{T_s} + [2d(t)\cdot B_1 + (1-2d(t)\cdot B_2]\langle u(\tau)\rangle_{T_s}. \quad (11)$$

The same analysis method is applied to the output average state vector. The expression of the average output vector can be inferred for:

$$\langle y(t)\rangle_{T_s} = [2d(t)\cdot \mathrm{C}_1 + (1-2d(t)\cdot \mathrm{C}_2]\langle x(t)\rangle_{T_s} + [2d(t)\cdot \mathrm{E}_1 + (1-2d(t)\cdot \mathrm{E}_2]\langle u(\tau)\rangle_{T_s}. \quad (12)$$

4 Small signal separation and linearization

In order to further determine static working point of the push-pull bi-directional DC-DC converter, and analyse the working condition of the AC small signal on the static working point, the state average variables need to be decomposed. The state average variables are decomposed into DC and AC small signal component. So the state average variables $\langle x(t)\rangle_{Ts}$, $\langle u(t)\rangle_{Ts}$ and $\langle y(t)\rangle_{Ts}$ can be resolved as follows:

$$\begin{cases}\langle x(t)\rangle_{T_s} = X + \hat{x}(t)\\ \langle u(t)\rangle_{T_s} = U + \hat{u}(t),\\ \langle y(t)\rangle_{T_s} = Y + \hat{y}(t)\end{cases} \quad (13)$$

where X is the DC component vector of the state vector. U is the DC component vector of the input vector. Y is the DC component vector of the output vector. $\hat{x}(t)$ is the AC small signal component vector of the state vector. $\hat{u}(t)$ is the AC small signal component vector of the input vector. $\hat{y}(t)$ is the AC small signal component vector of the output vector. At the same time, the control variable of the duty ratio $d(t)$ contains AC component, and it is decomposed of the DC component D and AC small signal component $\hat{d}(t)$. The expression is for:

$$d(t) = D + \hat{d}(t). \quad (14)$$

The state average vectors of the push-pull bidirectional DC-DC converter meet the small signal hypothesis, namely the amplitudes of each AC small signal component are far less than the amplitudes of the DC component. After the merger of similar items, the expression is for:

$$\langle \dot{x}(t)\rangle_{T_s} = [2DA_1 + (1-2D)A_2]X + [2DB_1 + (1-2D)B_2]U + [2DA_1 + (1-2D)A_2]\hat{x}(t) + [2DB_1 + (1-2D)B_2]\hat{u}(t) + [(2A_1 - 2A_2)X + (2B_1 - 2B_2)U]\hat{d}(t) + (2A_1 - 2A_2)\hat{x}(t)\hat{d}(t) + (2B_1 - 2B_2)\hat{u}(t)\hat{d}(t), \quad (15)$$

$$\langle y(t)\rangle_{T_s} = [2DC_1 + (1-2D)C_2]X + [2DE_1 + (1-2D)E_2]U + [2DC_1 + (1-2D)C_2]\hat{x}(t) + [2DE_1 + (1-2D)E_2]\hat{u}(t) + [(2C_1 - 2C_2)X + (2E_1 - 2E_2)U]\hat{d}(t) + (2C_1 - 2C_2)\hat{x}(t)\hat{d}(t) + (2E_1 - 2E_2)\hat{u}(t)\hat{d}(t), \quad (16)$$

where the DC and AC components are corresponding equal on either side of the equals sign. When the DC items are corresponding equal, can be deduced:

$$\begin{cases}\dot{X} = [2DA_1 + (1-2D)A_2]X + [2DB_1 + (1-2D)B_2]U\\ Y = [2DC_1 + (1-2D)C_2]X + [2DE_1 + (1-2D)E_2]U\end{cases}. \quad (17)$$

When the converter is on the steady state, the DC component X of the state vector is constant. So the static work point is solved in push-pull bidirectional DC-DC converter. The static work point is for:

$$\begin{cases}X = -A^{-1}BU\\ Y = (E - CA^{-1}B)U\end{cases}, \quad (18)$$

where $A = 2DA_1 + (1-2D)A_2$, $B = 2DB_1 + (1-2D)B_2$, $C = 2DC_1 + (1-2D)C_2$, $E = 2DE_1 + (1-2D)E_2$.

When the AC items are corresponding equal, it can be deduced:

$$\dot{\hat{x}}(t) = A\hat{x}(t) + B\hat{u}(t) + [(2A_1 - 2A_2)X + (2B_1 - 2B_2)U]\hat{d}(t) + (2A_1 - 2A_2)\hat{x}(t)\hat{d}(t) + (2B_1 - 2B_2)\hat{u}(t)\hat{d}(t), \quad (19)$$

$$\hat{y}(t) = A\cdot\hat{x}(t) + B\cdot\hat{u}(t) + [(2C_1 - 2C_2)\cdot X + (2E_1 - 2E_2)\cdot U]\cdot\hat{d}(t) + (2C_1 - 2C_2)\cdot\hat{x}(t)\cdot\hat{d}(t) + (2E_1 - 2E_2)\cdot\hat{u}(t)\cdot\hat{d}(t), \quad (20)$$

Equation (19) is small signal state equation of push-pull bidirectional DC-DC converter. Equation (20) is small signal output equation of push-pull bidirectional DC-DC converter. But the above two equations are nonlinear equations. Therefore they are linearized in the vicinity of the static working point. The right side of the equal sign is the product of nonlinear small signal in Equations (19) and (20). When the push-pull bidirectional DC-DC converter meets the small signal assumption, the amplitude of small signal product term is far less than the rest of the equal right. Therefore the product terms of the equation can be omitted.

The method of linearization does not introduce large errors, in order to achieve the linearization of nonlinear small signal equations. Equations (19) and (20) are linearized. The linear small signal state equation and the linear small signal output equation are inferred.

$$\begin{cases} \dot{\hat{x}}(t) = A\hat{x}(t) + B\hat{u}(t) + [(2A_1 - 2A_2)X + (2B_1 - 2B_2)U]\hat{d}(t) \\ \hat{y}(t) = A\hat{x}(t) + B\hat{u}(t) + [(2C_1 - 2C_2)X + (2E_1 - 2E_2)U]\hat{d}(t) \end{cases}. \quad (21)$$

5 Conclusions

Aiming at the need to achieve two-way energy flow, a push-pull bidirectional DC-DC converter is designed. The topological structure of the converter circuit is analysed. The dynamic modelling of circuit is done by using the state space averaging method. The linearization method is implemented by the AC small signal analysis. The linear expressions of the state space representation are derived. The work lays the foundation for the design of the control model and the study of the converter characteristics in the future. The design of push-pull bidirectional DC converter has the advantages of simple structure and a small number switching devices. The circuit will be adapting to small and medium power applications.

Acknowledgements

This paper was supported by the nature science foundation of Shanxi Province in China (2013011023-1). The authors would like to thank Science and Technology Department of Shanxi Province for supporting the research fund.

References

[1] Cinar S M 2012 *Journal of Engineering Science and Technology Review* **5**(4) 30-4
[2] Hu X F, Gong C Y A 2012 *Proceedings of the Chinese Society for Electrical Engineering* **32**(15) 8-15
[3] Camara M B, Gualous H, Gustin F 2010 *IEEE Transactions on Industrial Electronics* **57**(2) 587-97
[4] Tong Y B, Wu T, Jin X M, Chen Y 2007 *Proceedings of the Chinese Society for Electrical Engineering* **27**(13) 81-6
[5] Chainarin E, Kamon J 2013 *Journal of Power Electronics* **13**(4) 626-35
[6] Zhang Z, Thomsen O C, Andersen M A E 2012 *IEEE Transactions on industrial electronics* **59**(7) 2761-71
[7] Hote Y V, Choudhury D R, Gupta J R P 2009 *IEEE transactions on power electronics* **24**(10) 2353-6
[8] Han D H, Lee Y J, Kwon W S, Bou-Rabee M A, Choe G-H 2012 *Journal of Power Electronics* **12**(3) 418-28

Authors

Hongjuan Zhang, born in September, 1974, Shanxi, China

Current position, grades: associate professor at Taiyuan University of Technology, Taiyuan City, China.
University studies: PhD degree in Mechanical and Electronic Engineering from Taiyuan University of Technology, Shanxi, China, in 2011.
Scientific interests: computer modelling, system computer modelling, software programming, energy saving control.
Publications: 10.

Long Quan, born in March, 1959, Shanxi, China

Current position, grades: Doctor, professor, doctoral supervisor, Institute Director of Mechanical and Electronic Engineering Research, Taiyuan University of Technology, Shanxi, China.
Scientific interest: computer modelling, system computer modelling and design, software programming, intelligent control on mechatronics engineering, fluid power transmission and control, energy saving control.
Publications: over 80.

Yan Gao, born in July, 1969, Shanxi, China

Current position, grades: lecturer at Taiyuan university of technology, Taiyuan City, China.
University studies: M.E. in automation and information engineering from Taiyuan University of Technology, Shanxi, China, in 1998.
Scientific interests: computer application, software programming, control theory and intelligent control
Publications: 10.